



Cite this: *Catal. Sci. Technol.*, 2019, 9, 6517

Fe₃O₄@L-Proline/Pd nanocomposite for one-pot tandem catalytic synthesis of (±)-warfarin from benzyl alcohol: synergistic action of organocatalyst and transition metal catalyst†‡

Sanjiv O. Tomer and Hemant P. Soni *

One-pot synthesis of (±)-warfarin, an anticoagulant, has been achieved from benzyl alcohol in a ‘green way’ by using a multicomponent catalyst. For the purpose, L-proline capped Fe₃O₄ nanoparticles (Fe₃O₄@L-proline NPs) were synthesized and metallic palladium was loaded on its surface (Fe₃O₄@L-proline/Pd NCs). The morphology, particle size and shape were studied by using FESEM and TEM analysis. The Pd present on the surface was responsible for oxidation of benzyl alcohol and its derivatives to the corresponding aldehyde *in situ*. This in turn, condensed with acetone to form the aldol condensation product, benzylideneacetone, at 70 °C due to the presence of the L-proline organocatalyst on the surface of Fe₃O₄ NPs. Later, 4-hydroxycoumarin was introduced to condense with *in situ* generated benzylideneacetone by a Michael addition to form the target product (±)-warfarin. It was established that benzyl alcohol can be converted into the final product, (±)-warfarin, with an overall 35% yield within 5 days in a single-pot process. This process requires a rise in temperature in stages to a maximum of 100 °C and 1 atm pressure of dioxygen gas. An important aspect of the developed process is the avoidance of loss of costly Pd by leaching and catalyst recovery by the use of a magnetic field. The use of a solvent like PEG-400 makes the process green in a true sense. The interaction of L-proline with Fe₃O₄ NPs and the presence of Pd on the surface were confirmed by the FTIR and XRD patterns, respectively. The present study hereby suggests a combined 3-step mechanism for the production of the target product warfarin. Pilot-scale one-pot production of (±)-warfarin was carried out and a flow diagram with various unit processes is presented.

Received 27th July 2019,
Accepted 12th October 2019

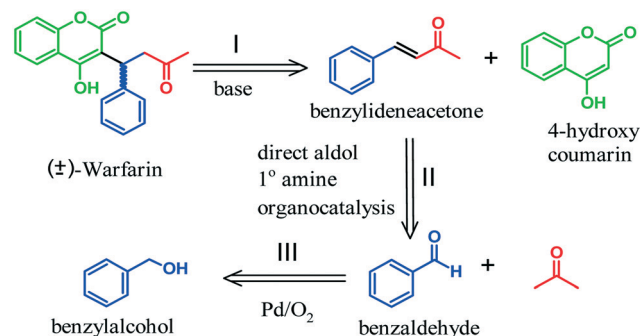
DOI: 10.1039/c9cy01497g

rsc.li/catalysis

1. Introduction

Warfarin (Coumadin® or Marevan®) is an anticoagulant drug most commonly prescribed by physicians for the prevention of thrombosis and embolism. It functions by inhibiting the vitamin K-mediated biosynthetic pathway leading to the formation of blood clotting proteins. Most commonly, it is synthesized by Michael addition of 4-hydroxycoumarin to benzylideneacetone in the presence of a base. Various organocatalysts having primary amines, amino acid functionalities and natural cinchona-derived chiral amines and diamines are reported to favor the asymmetric synthesis

of one of the enantiomers.^{1–4} The *S*-enantiomer is shown to be 2–5 times more active than the *R*-enantiomer. Moreover, it has a different metabolic pathway in humans and also has a shorter half-life than the *R*-enantiomer (21–40 h for *S*- and 37–89 h for *R*-warfarin).^{5–7} However, in general, it is



Scheme 1 Planning for one-pot synthesis of (±)-warfarin from benzyl alcohol through 3-way catalysis by using a single nanocomposite catalyst having multiple components (I, II and III).

Department of Chemistry, Faculty of Science, The Maharaja Sayajirao University of Baroda, Vadodara-390 002, Gujarat, India. E-mail: drhpsoni@yahoo.co.in; Tel: +91 0265 2795552

† This work is dedicated to Dr. D. P. Bharambe, a humble teacher and mentor, on the occasion of his 62nd birthday and retirement.

‡ Electronic supplementary information (ESI) available: XRD patterns, TEM images with SAED pattern, FTIR spectra of all synthesized materials, synthesis scheme, combined reaction mechanism, ¹H NMR and ¹³C NMR are provided in the ESI. See DOI: 10.1039/c9cy01497g

prescribed in the racemate form^{1,5} and its dosage is adjusted on an 'individual basis' considering the patient's disease history. Herein, we have attempted to synthesize (±)-warfarin from scratch in a one-pot synthesis by 3-way catalysis, that is, by (i) oxidizing benzyl alcohol to aldehyde and then (ii) condensing the latter with acetone directly in an aldol fashion leading to benzylideneacetone; (iii) it is then condensed with 4-hydroxycoumarin resulting in the target racemic product (Scheme 1) by developing a catalytic nanocomposite. A properly designed nanocomposite material can do its function effectively and efficiently ranging from hydrodesulfurization of liquid fuels, photocatalysis, and catalysis in organic transformations to magnetic resonance imaging and photothermal ablation therapy.^{8–12}

Controlled oxidation of benzyl alcohol to benzaldehyde is very well reported in the literature.^{13,14} Many oxidizing agents are explored for the purpose. For example, a stoichiometric quantity of Cr(vi) (John's reagent, Collins reagent, PCC, PDC *etc.*), Mn(vii) (aqueous, acidic or basic solution of KMnO₄), Os(viii) (OsO₄), and Ru(vi, viii) (RuO₄) metal-based reagents are all used for the purpose.¹⁵ Attempts have also been made to use H₂O₂ or O₂ as an oxidant for a neat, clean and atom-efficient oxidation process.^{16–20} These oxidants work in the presence of early transition metals with d⁰ configuration like Mo(vi), W(vi), Ti(v) or Pd(ii) complexes. However, these methods involve chlorinated solvents and generate metallic salts as solid waste that are toxic and pollute the environment. Oxidation methods mediated by TEMPO (2,2,6,6-tetramethylpiperidine-1-yloxy) and related stable nitroxide radicals (Anelli oxidation)²¹ have also been developed. However, these methods contain bleach (NaOCl) and HOCl which are generated *in situ* that harm the environment.²² Hence, the development of neat, clean and atom efficient oxidation processes are the need of the day.^{23,24} From the mechanistic points of view, the above oxidizing agents donate an O atom, an intrinsic part of their molecular structure, to the substrate and oxidize it. However, the same function can be carried out by using pure O₂, air or peroxides (H₂O₂ is desirable) as an oxidant for 'green' oxidation processes. However, molecular oxygen in the ground state (triplet state) is 'inactive' and needs to be activated to act as an oxidizing agent.²⁵ This requires early transition metals with d⁰ configuration (as mentioned above) and their complexes with sterically hindered ligands like PPh₃ mediated catalysis. For example, R. A. Sheldon's group developed a water-soluble Pd(ii) bathophenanthroline complex for selective aerobic oxidation of a wide range of alcohols to aldehydes, ketones and carboxylic acids in a biphasic water–alcohol system. The use of water as a solvent and air as the oxidant made the process economical and environment friendly.²⁰ However, as the catalyst is water soluble, there is a chance of loss of precious Pd metal during catalyst recovery. A number of efforts have been made on Au-based materials for alcohol oxidation. For example, T. Saleh's group developed a series of NCs made of Pd and Au NPs supported on carbon (Au–Pd/C), prepared by impregnation

and solvent immobilization techniques.²⁶ These catalytic NCs were evaluated for solvent-less oxidation of benzyl alcohol to benzaldehyde in the liquid phase by using 35% H₂O₂ as an oxidizing agent. They were able to achieve 88% selectivity for the target oxidation in the presence of Au–Pd/C NCs prepared by the impregnation method. Enache *et al.* developed a Au@Pd core–shell supported on a TiO₂ matrix for oxidation of a 1° alcohol to aldehyde with O₂ as the oxidant at 373 K. They obtained a very high TOF (270 000 per h) from the process.²⁷ However, it is too costly and commercially unviable. It is established that the recovery of Pd becomes efficient when it is anchored/doped/supported on a solid matrix which is magnetic or superparamagnetic in nature. Zamani *et al.* reported a Pd/Fe₃O₄/amino acid nanocomposite. They obtained more than 99% selectivity for benzyl alcohol to benzaldehyde under solvent-free conditions.²⁸ Wang *et al.* prepared Pd supported on Al₂O₃ and TiO₂ by a wet impregnation method and used it as a catalyst for solvent-free selective oxidation of benzyl alcohol by molecular oxygen. The developed catalyst showed high activity and selectivity for benzaldehyde on pretreatment like calcination.²⁹

Drawing inspiration from these studies and considering the need for the recovery of the precious metal catalyst without any loss, it was planned to load the metallic Pd on the surface of magnetic Fe₃O₄ nanoparticles (NPs) in the present study.

Generally, aldol condensation requires a base (dil. NaOH) catalyst and activation of substrates to react in a desired way to form the C–C bond.^{30,31} It takes place in two steps, namely, aldolization and dehydration. Practically, with a stronger base, high temperature and longer reaction time, the aldol product can become dehydrated to form an α,β -unsaturated carbonyl compound. The development of a direct catalytic asymmetric aldol reaction (limited to the first step) under mild conditions in the presence of L-proline like amino acids as organocatalyst,³² aldolase enzyme³³ or catalytic antibodies³⁴ in a 'green solvent' like water is a subject of research and reported very well in the literature. For the present, required strategy for the one-pot synthesis of warfarin, an aqueous solution of base cannot be used due to its chance of attacking the Fe₃O₄ host matrix. List, Lerner and Barbas reported for the first time an enamine-based organocatalyst for asymmetric aldol reaction.³⁵ Encouraged by this, a strategy was devised such that L-proline can be loaded onto the surface of Fe₃O₄ either by using a carboxylic acid group as a 'handle' or by H-bonding with a surface oxygen atom, leaving the secondary imine group, the catalytic site, free. The loading of L-proline onto the Fe₃O₄ surface would serve two purposes: (i) it would provide a catalytic site for the aldol reaction which can further proceed to α,β -unsaturated ketone by adjusting the time and temperature of the reaction; (ii) it can also serve as a base required in a catalytic amount for final condensation with 4-hydroxycoumarin in step III (Scheme 1).

It can be concluded from the above discussion that for the development of a green one-pot tandem catalytic process for the production of (\pm)-warfarin from benzyl alcohol, the following parameters should be taken care of: (i) sufficient Pd sites should be available on the surface of the magnetic matrix; (ii) there are chances of formation of by-products like carboxylic acid, esters, or ethers in the first step, dibenzylideneacetone (dimer) in the second step and other condensation products in the third step, which should not interfere during the reaction or in the preceding steps; (iii) there should be an immediate desorption of products from the surface and should not block the catalytic sites; (iv) the product of the first step should easily be available as a reactant for the second step and so on for the continuation of the tandem process; (v) the selection of the solvent system for this tandem process is crucial and it should be compatible with all the reaction components and should be green in nature as well as recyclable; (vi) corrosion of the matrix and leaching of the catalytic components should be monitored throughout the process. All these aspects can be set by process optimization. Overall, economic and ecological aspects should be considered for the development of the one-pot multi-stage organic transformations on the industrial scale.

The purpose of this work is to develop a tandem one-pot catalytic process involving a cascade of chemical reactions carried out by using 'green solvents and reagents' leading to racemic warfarin. For this, we have developed $\text{Fe}_3\text{O}_4@L$ -proline/Pd nanocomposite (NCs) and used it as single catalyst for the proposed tandem process beginning from benzyl alcohol. The process parameters like temperature, reaction time, solvent and the stoichiometry of the reagents required at each stage are optimized considering the environmental aspects.

2. Results and discussion

The synthesized *L*-proline capped Fe_3O_4 NPs were characterized by XRD to confirm the phase, purity, particle size and crystallinity of the material (Fig. S1 \ddagger). The XRD pattern manifests predominant diffraction peaks at 2θ values of 30.51° , 35.78° , 43.55° , 47.13° , 53.50° , 57.40° , 62.92° , 65.74° , 70.92° , 73.96° , 74.96° and 78.92° corresponding to the (220), (311), (400), (331), (422), (333), (440), (531), (620), (533), (622) and (444) planes, respectively (JCPDS 82-1533), confirming the magnetite phase of Fe_3O_4 (Fig. 1A). The magnetite phase is known for its inverted spinel structure having a face centered cubic (FCC) arrangement and Fe cations occupying the interstitial Td and/or Oh sites. The particle size was calculated from the Debye-Scherrer formula ($L = 0.9\lambda/\beta \cos \theta$)³⁶ and the FWHM (full width at half maximum) value of the major peak for (311) planes in the range of 10 nm. There is no change in the XRD pattern due to the coating of an *L*-proline layer over Fe_3O_4 , suggesting only the surface interaction/adsorption of organic molecules.

On introduction of Pd in $\text{Fe}_3\text{O}_4@L$ -proline NPs, new peaks at 2θ values of 40.43° , 40.65° and 68.12° emerged corresponding to the (111), (200) and (220) planes of Pd, respectively (JCPDS 46-1043). The major peak at 40.43° due to the (111) planes has high intensity while the other two peaks are of low intensity due to a very small amount of Pd in the host matrix (Fig. 1A). This confirms that the Pd metal is in zero oxidation state (also, due to hydrazine, a reducing agent used to load Pd on the host matrix). The emergence of new peaks in the XRD pattern on loading Pd indicates the presence of Pd as a separate phase in the form of small islands on the host surface which can act as catalytic sites for organic transformations. The nitrogen adsorption-desorption isotherms for the synthesized $\text{Fe}_3\text{O}_4@L$ -proline NPs and $\text{Fe}_3\text{O}_4@L$ -proline/Pd NCs, their calculated BET surface area and pore volume are presented in Fig. 1(B and C) and Table 1. It can be observed from Fig. 1 that the isotherms of $\text{Fe}_3\text{O}_4@L$ -proline NPs are almost similar to that of type IV (BDDT classification) with the H4 type of hysteresis loop in which the two branches are nearly horizontal and parallel over a wide range of relative pressures (P/P^0). The quantity of gas adsorbed, in this case, increases with increase in P/P^0 . The type H4 loop is often associated with narrow slit-like pores.^{37,38} The adsorption average pore width ($4 V \text{ \AA}^{-1}$ by BET) values indicate a mesoporous material. It can be observed from Table 1 that on loading Pd, the BET surface area increases. The BET surface area and pore size studies reveal that the material is suitable for catalytic activities. N_2 adsorption-desorption analyses could not provide structural and morphological information about the material. Therefore, the structure and morphology of the samples were directly observed by field effect scanning electron microscopy (FESEM) and transmission electron microscopy (TEM). Fig. 1(D and E) show FESEM images of $\text{Fe}_3\text{O}_4@L$ -proline NPs and $\text{Fe}_3\text{O}_4@L$ -proline/Pd NCs. They indicate a spherical morphology, and on loading Pd, the surface area and porosity of the material increase while maintaining the morphology, supporting the BET results. The TEM images for pristine Fe_3O_4 , $\text{Fe}_3\text{O}_4@L$ -proline NPs and $\text{Fe}_3\text{O}_4@L$ -proline/Pd NCs also show spherical particles and are in the size range of 10–15 nm (Fig. 1F and G and S2 \ddagger). The spots having equal intensity in selected area electron diffraction (SAED) indicate the highly crystalline nature of the material. The lattice fringes of the exposed (200) planes of magnetite present in $\text{Fe}_3\text{O}_4@L$ -proline/Pd are at 0.15 nm distances each and that for Pd at 0.25 nm, corresponding to (111) planes. From the TEM images and SAED patterns it can be concluded that the *L*-proline organic layer and Pd loading did not alter the lattice parameters of the host Fe_3O_4 , retaining the crystallinity of the material which is necessary for the catalytic activity and recycling ability due to the magnetic nature of the material. TEM in combination with EDS elemental mapping analysis was employed to determine the distribution of elements in the

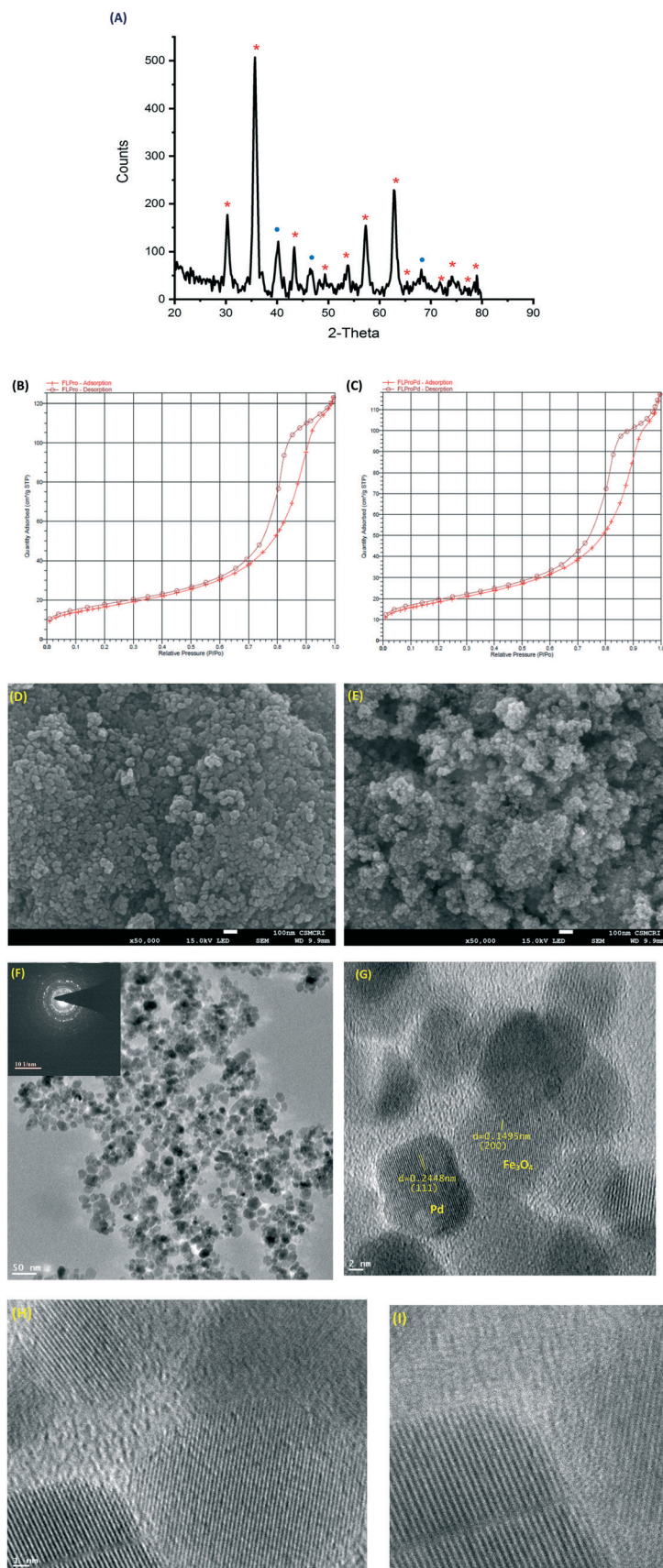


Fig. 1 (A) XRD pattern of $\text{Fe}_3\text{O}_4@L\text{-proline}/\text{Pd}_2$ NCs (* and • indicate Fe_3O_4 and Pd respectively) (B and C) nitrogen adsorption–desorption isotherms for $\text{Fe}_3\text{O}_4@L\text{-proline}$ and Pd loaded $\text{Fe}_3\text{O}_4@L\text{-proline}$ (D) FESEM image (before Pd loading) (E) FESEM image (after Pd loading) (F) TEM image (inset image shows SAED pattern) and (G–I) lattice fringes at higher magnification of as-synthesized $\text{Fe}_3\text{O}_4@L\text{-proline}/\text{Pd}_2$ NCs.

Table 1 BET surface characterization of as-synthesized NPs and NCs

Sr. no.	Parameters	Fe ₃ O ₄ @L-proline NPs	Fe ₃ O ₄ @L-proline/Pd2 NCs
1	S_{BET} (m ² g ⁻¹)	59.39	65.23
2	Average pore diameter (Å)	114.99	111.67
3	Adsorption average pore width (4 V Å ⁻¹ by BET) (Å)	127.94	111.20
4	Pore volume (cm ³ g ⁻¹)	0.19	0.18
5	Total volume in pores (cm ³ g ⁻¹)	0.17 (by DFT)	0.16 (by DFT)
6	Total area in pores (m ² g ⁻¹)	36.75 (by DFT)	34.68 (by DFT)

Fe₃O₄@L-proline/Pd nanocomposite. The results are given in Fig. 2. The images clearly show the uniform distribution of Pd metal on the surface of the Fe₃O₄ host.

FTIR spectroscopy is one of the best tools to study the interaction of ligand molecules with the host surface atoms.^{39–41} Fig. S3† shows the FTIR spectrum of L-proline. The vibrations at 1622 and 1428 cm⁻¹ correspond to ν_{as} and ν_{s} carboxylate stretching, respectively, while the hump at 1335 cm⁻¹ corresponds to -OH bending in carboxylic acid when it is in the free form. When L-proline interacts with Fe₃O₄, this hump disappears (Fig. S3†), keeping other carboxylate stretching vibrations intact (Fig. S3†) and suggesting that L-proline molecules orient on the surface of Fe₃O₄ by H-bonding with surface oxygen atoms (Fig. 3). The vibration at 636 cm⁻¹ is due to Fe–O stretching. There is no

subtle change in FTIR spectra when Pd is loaded on Fe₃O₄@L-proline.

As discussed earlier, 3-way catalysis is required for the one-pot synthesis of (±)-warfarin from benzyl alcohol. The benzylideneacetone formed by α -alkylation of ketone with a 1° alcohol in two steps can be directly condensed with 4-hydroxycoumarin under mild basic condition in a single pot. For this purpose, the amount of L-proline and Pd loaded onto the surface of the host Fe₃O₄ must be optimized. A stoichiometric amount of L-proline was used as a capping agent during the synthesis of Fe₃O₄ NPs. Hence, the amount of Pd loaded on the surface of Fe₃O₄@L-proline was varied. Accordingly, three sets of Fe₃O₄@L-proline/Pd NCs were prepared (Scheme S1†) and used for optimization of the alcohol/ketone condensation reaction leading to

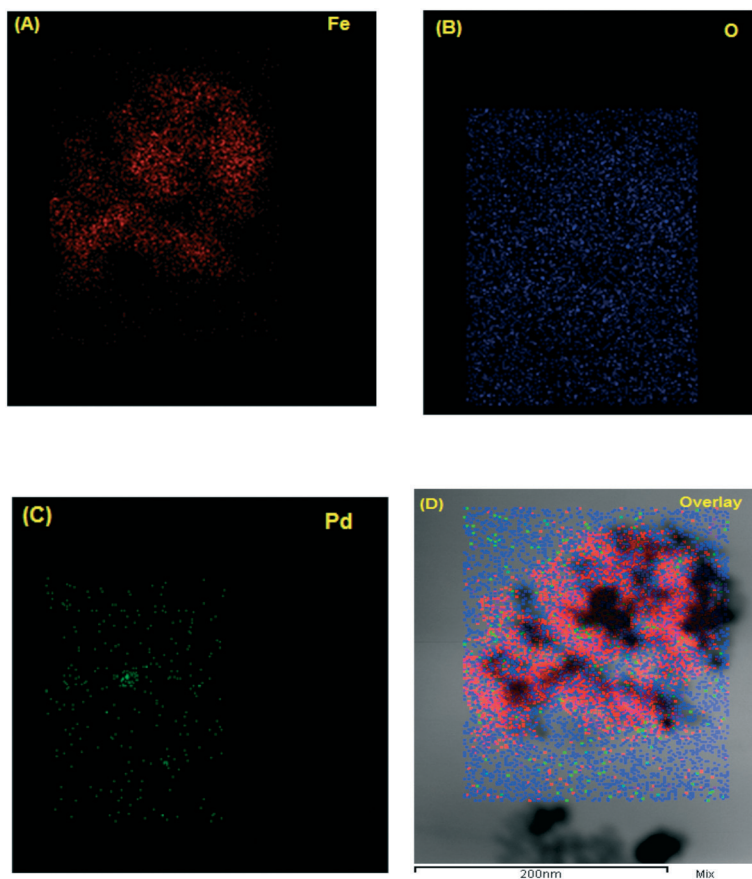


Fig. 2 Elemental distribution analysis of Fe₃O₄@L-proline/Pd2 NCs, elemental mapping of (A) Fe (red), (B) O (blue), (C) Pd (green) and (D) their overlay.

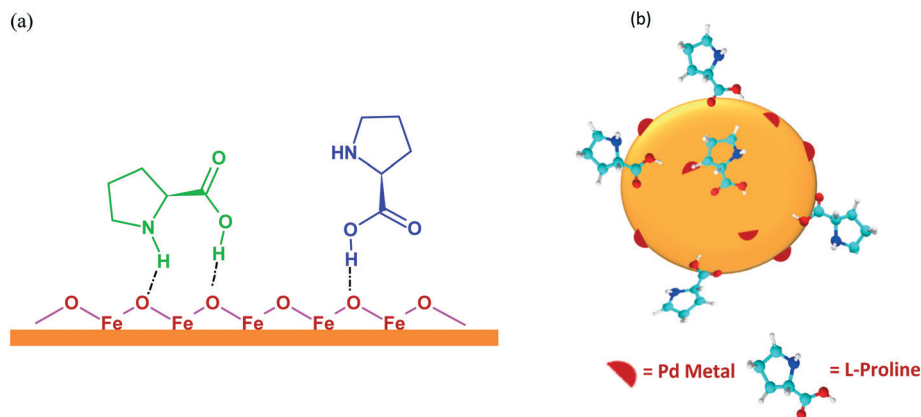


Fig. 3 Interaction of L-proline molecules with the Fe_3O_4 NPs' surface (a) through H-bonding, revealed from FTIR spectroscopy and (b) cartoon showing the overall molecular framework of the multicomponent catalyst deduced from FTIR spectroscopy and XRD analysis. Small dark-brown semi-spheres show Pd islands on the surface of host Fe_3O_4 NPs (dark yellow).

benzylideneacetone in one pot. The amount of Pd loaded was also determined from elemental EDAX analysis (Fig. S4†).

It can be observed from Table 2 that $\text{Fe}_3\text{O}_4@L\text{-proline}/\text{Pd}1$ having the maximum amount of Pd loaded (A, 500 mg g^{-1} NPs) can convert 1 to 2 in 32 h in the presence of O_2 gas at 1 atm and 60 °C in PEG-400 medium, but it failed to transform 2 into 3 in a separate reaction. This may be due to the blocking of the catalytic imine site of L-proline with excess Pd. When $\text{Fe}_3\text{O}_4@L\text{-proline}/\text{Pd}3$ NPs having a lesser amount of Pd loaded (C, 50 mg g^{-1} NPs) was used as a catalyst, the first conversion, 1 to 2, could not take place in a measurable amount while it could convert 2 to 3 within 20 h when the reaction was carried out separately. Optimum performance could be achieved in the presence of $\text{Fe}_3\text{O}_4@L\text{-proline}/\text{Pd}2$ (B, 200 mg Pd per g NPs); it was able to transform 1 to 2 in 60 h and 2 to 3 in 24 h in separate reactions. Hence, $\text{Fe}_3\text{O}_4@L\text{-proline}/\text{Pd}2$ was selected to proceed further.

2.1 Screening of solvent

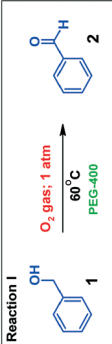
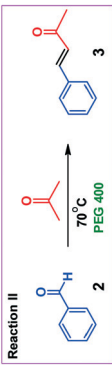
Both the processes, namely, oxidation of benzyl alcohol to benzaldehyde (1 to 2, reaction I) and condensation of benzaldehyde with acetone to benzylideneacetone (2 to 3, reaction II), were carried out separately in the presence of as-synthesized NCs as catalyst for solvent screening to achieve optimum conversion by considering the 'green aspects'. The best choice for the purpose is to carry out the transformations in water as a medium. It can be observed from Table 3 that reaction I was successfully carried out in water, and about 70% yield of 2 was achieved in 96 h at RT; however, no reaction took place for reaction II in water at RT up to 70 °C. Similar results were obtained when both the reactions were carried out in toluene as a solvent. Also, both the reactions were unable to proceed separately at RT in ethanol as the reaction medium. We had also carried out the reactions in PBS buffer at neutral pH 7.4. Interestingly, 76% conversion was achieved at RT within 60 h for reaction I; however, it was unable to support reaction II separately

although it continued up to 2 days. In a literature survey, we found that PEG-400 is a low cost, non-toxic and eco-friendly liquid polymer and in addition, it can be recovered by extraction with a suitable solvent or by direct distillation of water or solvent.^{42,43} It can act as a recyclable reaction medium for the Baylis–Hillman reaction,⁴⁴ Heck reaction⁴⁵ and asymmetric dehydroxylation.⁴⁶ It also supports the aldol condensation reaction by acting as a catalyst with anhydrous K_2CO_3 .⁴⁷ S. Chandrasekhar *et al.* reported an L-proline catalyzed asymmetric aldol reaction in PEG-400 as a recyclable medium.⁴⁸ They were able to recycle this solvent 10 times without losing the activity of the L-proline catalyst. In the present case, when PEG-400 was used as a solvent for reaction I, it was unable to support the oxidation of 1 to 2 at RT although the reaction was continued for 4 days; however, it could complete the reaction at 60 °C to almost 90% conversion within 3 days (Table 3). Similar results were observed for reaction II for aldol condensation of 2 to 3 with acetone (Table 4). PEG-400 was not able to sustain this reaction at RT up to 40 °C when the reaction was continued for 2 days, but could drive the reaction to 53% yield at 70 °C within 24 h (Table 4). Hence, it is established that PEG-400 is suitable as a solvent for one-pot α -alkylation of acetone with benzyl alcohol. It can be assumed that reaction II may proceed *via* β -hydroxyketone, but it directly converted into 3 due to dehydration at high temperature.

2.2 Screening of substrate

Different derivatives of benzyl alcohol were evaluated for both reactions I and II separately to understand the electronic effect of substituent groups on the reaction (Tables 5 and 6). *p*-Nitrobenzyl alcohol could not undergo oxidation under optimized reaction parameters (O_2 , 1 atm/60 °C, PEG-400) and resulted in poor yield (15%) in 3 days while 53% yield was obtained for reaction II under optimized parameters (acetone, 70 °C, PEG-400) in 2 days. When the electron releasing $-\text{OH}$ group was attached to benzyl alcohol, reaction

Table 2 Reaction optimization in the presence of as-synthesized catalytic nanocomposite having different amounts of Pd loading^{a,c}

Catalyst system	Amount ^b of Pd mg g ⁻¹ NCs	Reaction I	Reaction II
A	500		
B	200	Reaction completed in 60 h No reaction	No reaction Reaction completed in 24 h Reaction completed in 20 h
C	50	No reaction	No reaction

^a Aerial oxygen is not sufficient to complete the reaction I. ^b Theoretical amount. Actual amount varies in the same proportion as determined from EDX elemental analysis (Fig. S4). ^c The progress of the reaction was monitored on the TLC plate after every 4 h and the reactions were carried out in triplicate.

I was completed within 60 h with almost 90% yield. However, it was unable to carry out aldol condensation even though the reaction was continued for 2 days. It is interesting to note that *p*-OCH₃, *p*-CH₃ and *p*-Cl attached to benzyl alcohol can undergo both the reactions (separately) with substantial percentage yields (entries 4–6, Tables 5 and 6) in 60 and 24 h for reactions I and II, respectively. Unsubstituted benzyl alcohol undergoes oxidation with the highest (94%) yield in 60 h, while its corresponding aldehyde can condense with acetone at 70 °C in PEG-400 medium to form 3 within 24 h and with 53% conversion in a separate reaction (entry 2, Tables 5 and 6).

From the above observations, benzyl alcohol was selected to begin with, to carry out both reactions I and II in a single pot in the presence of Fe₃O₄@l-proline/Pd₂ NCs as the catalyst and PEG-400 as the solvent. It can be seen from Table 7 that benzyl alcohol yields the corresponding benzylideneacetone at the end of the 4th day with 47% yield, while *p*-CH₃, *p*-Cl and *p*-OCH₃ derivatives of 1 yield 52%, 52% and 58% overall conversion to 3, respectively, at the end of the 4th day in one pot.

In next set of experiments, the above two steps were extended to the third sequential reaction, that is, the Michael addition of 4-hydroxycoumarin (4) to 3. The pot reaction was extended for a further 12 h at 100 °C maintaining the other pot conditions the same (Scheme 2). At the end of the 5th day (overall 120 h), (±)-warfarin could be separated by fractional crystallization from the reaction mass with 35% yield. The peculiarity of this one-pot one catalyst process is that the solvent PEG-400 can be recycled (3 times in this study) to carry out fresh pot reactions without the loss of catalytic activity.

2.3 Discussion

Park *et al.*⁴⁹ reported palladium (0.2 mol%) nanoparticles entrapped in aluminium hydroxide, Pd/AlO(OH). This catalyst shows activity for alkene hydrogenation and aerobic alcohol oxidation. It produced 1,3-diphenylpropan-1-one (6) in 97% yield in α -alkylation of acetophenone 5 with 1.2 equiv. of 1 in the presence of a base like K₃PO₄ (3 equiv.) for 8 h at 80 °C under argon (Scheme 3). It produced chalcone 8 with a yield of 95% in 20 h when the reaction was carried out under 1 atm O₂ in a toluene medium. They compared the activity of the catalyst with different commercially available combinations like 5% Pd/C, 5% Pd/Al₂O₃, 5% Pd/BaCO₃, [RuCl₂(PPh₃)₃], [Ir(cod)Cl]₂ etc. However, these catalysts favor 6 as the major product with very little formation of 7. Product 8 was obtained in trace amounts or even none at all. In contrast, the herein developed catalyst favors 8 as the major product due to step-wise reactions.

Further, these catalytic processes require a base like K₃PO₄ (3 equiv.) or KOH (1 to 0.1 equiv.) for each cycle to achieve the optimum reaction rate again. Such strong bases may attack the host surface responsible for leaching of the precious metal catalyst. The Ru grafted hydrotalcite was reported to bring about

Table 3 Optimization of solvent system and temperature for reaction I in the presence of as-synthesized Fe₃O₄@L-proline/Pd2 NCs

Reaction I

Solvent	Time ^c (h)	Temperature (°C)	Yield ^{a,b} (%)
Toluene	48	70	56
Ethanol	48	RT	Trace
PBS buffer pH 7.4	60	RT	76
Water	96	RT	70
PEG-400	96	RT	Trace
PEG-400	60	60	94

^a Isolated yields after column chromatography. The reactions were carried out in triplicate. ^b Benzyl alcohol (1.0 mmol), solvent (5 mL) and catalyst (100 mg) were stirred at the above-mentioned temperature under 1 atmosphere pressure of dioxygen in a sealed tube till the disappearance of the starting material (from the TLC plate). The product was extracted in diethyl ether (10 mL × 3), concentrated and purified by column chromatography eluting with cyclohexane/ethyl acetate. ^c The progress of the reaction was monitored on the TLC plate after every 4 hours.

Table 4 Optimization of solvent system and temperature for reaction II in the presence of as-synthesized Fe₃O₄@L-proline/Pd2 NCs

Reaction II

Solvent	Time (h)	Temperature (°C)	Yield ^{a,b} (%)
Toluene	24	70	No reaction
Ethanol	24	RT	No reaction
PBS buffer pH 7.4	24	RT	No reaction
PBS buffer pH 7.4 + DMSO	24	RT	No reaction
Water	24	RT	No reaction
Water	24	39	16
PEG 400	24	40	Trace
PEG 400	24	70	53

^a Isolated yields after column chromatography. The reaction was carried out in triplicate for 24 h and the progress of the reaction was monitored on the TLC plate after every 4 hours. ^b Benzaldehyde (1.0 mmol), acetone (5 mL), and catalyst (100 mg) in 5 mL of the above solvent were stirred at ambient temperature in a sealed tube till the disappearance of the starting material (from the TLC plate). The product was extracted in diethyl ether (10 mL × 3), concentrated and purified by column chromatography eluting with cyclohexane/ethyl acetate.

α -alkylation of ketone to produce 6 without any requirement of a base. However, it demands a very high temperature of 180 °C.⁵⁰ Yanan *et al.* have reported α -alkylation of acetone with 1 in the presence of CrO₃ at 56 °C in 10 h.⁵¹ Apart from benzyl alcohol, they selected *p*-OCH₃ and *p*-Cl derivatives as substrates and achieved a high percentage yield of benzylideneacetone, in agreement with our present results. They also obtained dibenzylideneacetone as a by-product in various proportions. In this case, CrO₃ worked as the oxidant as well as the catalyst and was consumed at the end of the reaction. Hence, from the environmental point of view, this catalyst cannot be used in an industrial scale. The importance of the presently developed catalyst is that it can do 3-way catalysis leading to (\pm)-warfarin in a single-pot process in the presence of all the products, by-products and intermediates generated during various reaction steps. The mechanism combining transition metal catalysis and organocatalysis is shown in Fig. S5.†

It is quite natural to think of chiral induction during step 3 of the tandem process due to the presence of L-proline on the surface as a 2° amine organocatalyst to form enantiopure (*R*)- or (*S*)-warfarin. Kristensen *et al.*⁵² had tested most common organocatalysts like the MacMillan-type imidazolidinone (9) and the Jørgensen/Hayashi diarylprolinols (10, 11 Fig. 4) for the synthesis of enantiopure warfarin. They achieved an excellent percentage yield of racemic warfarin but poor conversion to a single specific stereoisomer even after 9 days. The Jørgensen group¹ also carried out this reaction in the presence of *S*-proline but they obtained only racemic warfarin as the product. The possible reason, as explained by Kristensen, may be the long reaction time due to which the racemic pathway dominates over the asymmetric one.⁵²

To extend the application of the synthesized catalyst NCs and the developed one-pot tandem reaction, we had carried

Table 5 Oxidation of benzyl alcohol and its derivatives to the corresponding aldehyde (reaction 1) under optimized reaction parameters in the presence of $\text{Fe}_3\text{O}_4@L\text{-proline}/\text{Pd}2\text{ NCs}^a$

$\text{1} \xrightarrow[\text{PEG 400}]{\text{Fe}_3\text{O}_4@L\text{-proline}/\text{Pd } 2, \text{ O}_2; 1 \text{ atm}/60 \text{ }^\circ\text{C}}$ 2

Sr. no.	-R	Time (h)	Product	Yield (%)
1	-NO ₂	60		15
2	-H	60		94
3	-OH	60		90
4	-CH ₃	60		92
5	-Cl	60		80
6	-OCH ₃	60		78

^a The detailed protocol is discussed in the Experimental section.

out the reaction in a pilot plant. The flow diagram of the unit processes used for the production of (\pm)-warfarin starting from 10 g of benzyl alcohol is shown in Fig. 5.

The procedure used for the production of the target product in a tandem process in a pilot plant is discussed in detail in the Experimental section.

3. Conclusion

We have demonstrated that multi-step synthesis of pharmaceutically important molecules can be carried out in a single pot by inserting multiple catalytic components into a robust host and optimizing the reaction parameters. Various catalytic components present in a single nanocomposite work synergistically such that organic transformations, like oxidation of benzyl alcohol to benzaldehyde (Pd metal as catalyst), which in turn later condensed with acetone in an aldol fashion (*L*-proline as organocatalyst) resulting in benzylideneacetone which then condensed with 4-hydroxycoumarin by Michel addition (*L*-proline, as secondary amine, provides the basic condition) leading to the target product warfarin, are carried out in a synchronized way. By implementing all the optimized process parameters for the pilot-scale production of (\pm)-warfarin, it can be concluded that (i) the developed process becomes cost-effective compared to others based on bare noble metal catalysts; (ii) the catalyst recovery becomes easy by applying a magnetic field; (iii) the possibility of noble metal leaching from NCs is nullified in the process as no strong base is used

at any stage; (iv) the as-synthesized catalyst NCs maintained their efficiency for three cycles (under this study) for 3-way catalysis; (v) the reaction is 'green' as no noxious solvents are used and the whole one-pot process can be carried out in PEG-400 and water as the reaction medium. This study opens new avenues for the development of multicomponent catalysts to produce materials on a large scale in a 'green way'. The next study would be the development of a tandem process for the large-scale production of enantiopure warfarin by loading chiral 1° diaryldiamines on the magnetic host surface with palladium.

4. Experimental

All the chemicals were purchased from Aldrich Chemicals unless specified. $\text{FeCl}_3 \cdot 6\text{H}_2\text{O}$ was purchased from Loba Chemie, India. $\text{FeSO}_4 \cdot 4\text{H}_2\text{O}$ was purchased from S. D. Fine Chemicals Limited, India. Aqueous ammonia was purchased from S. R. Enterprise, India. *L*-Proline was purchased from TCI Chemicals and palladium acetate from Hindustan Platinum.

4.1 Synthesis of *L*-proline coated magnetic nanoparticles ($\text{Fe}_3\text{O}_4@L\text{-proline}$ NPs)

Amino acid-coated magnetite nanoparticles were synthesized by the one-pot synthesis method. In brief, ferric chloride hexahydrate (5.0 g, 18.5 mmol) and ferrous sulphate tetrahydrate (2.4 g, 10.7 mmol), molar ratio 1:0.58, were added to 250 mL deionized water under an inert atmosphere.

Table 6 Aldol condensation of benzaldehyde and its derivatives to the corresponding benzylideneacetone (reaction II) under optimized reaction parameters in the presence of $\text{Fe}_3\text{O}_4@\text{L-proline}/\text{Pd}2$ NCs^a

Sr. no.	-R	Time (h)	Product	Yield (%)
1	-NO ₂	24		No desired product
2	-H	24		53
3	-OH	24		No reaction
4	-CH ₃	24		58
5	-Cl	24		68
6	-OCH ₃	24		65

^a The detailed protocol is discussed in the Experimental section.

The mixture was heated to 70 °C to obtain a clear yellow solution. The mixture was stirred vigorously with a mechanical stirrer to avoid interparticle magnetic interaction. After 30 min, L-proline (5.3 g, 46.0 mmol) dissolved in 50 mL deionized water was rapidly added. The clear reaction mixture was further stirred for another 30 min. Then 27 mL ammonium hydroxide (25%) was rapidly added which in turn changed the reaction color to black. The stirring was continued for 1.5 h. Finally, the black nanoparticles were separated magnetically, washed with distilled water three times, and dried in an oven at 100 °C overnight. Dry weight of nanoparticles: 3.0 g.

4.2 Synthesis of palladium loaded amino acid functionalized magnetic nanocomposites ($\text{Fe}_3\text{O}_4@\text{L-proline}/\text{Pd}$ NCs)

Palladium acetate (0.2 g, 0.89 mmol) was dissolved in 200 mL of ethanol at room temperature with vigorous mechanical stirring to obtain an orange colored transparent solution. To this solution was added 1.0 g L-proline coated magnetic nanoparticles ($\text{Fe}_3\text{O}_4@\text{L-proline}$). This suspension was stirred vigorously and refluxed for 2 h. As the reaction proceeded, the initial brown suspension turned dark. This reaction mixture was cooled to room temperature and 2.5 mL 80% hydrazine hydrate was added. The reaction mixture was further refluxed for 1.5 h. The generated nanocomposites were separated magnetically, washed with ethanol three times followed by distilled water three times, and then dried

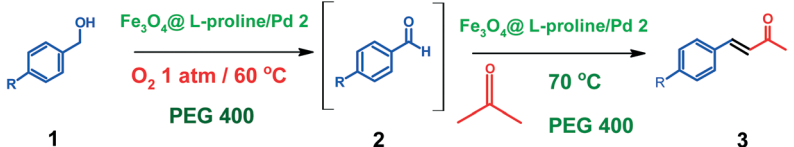
in an oven at 60 °C overnight. Dry weight of nanoparticles: 1.01 g.

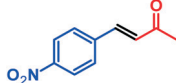
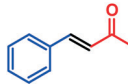
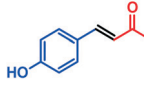
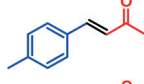
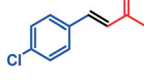
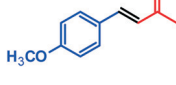
4.3 Oxidation of benzyl alcohol (1) to benzaldehyde (2)

Benzyl alcohol (100 mg, 0.92 mmol) and $\text{Fe}_3\text{O}_4@\text{L-proline}/\text{Pd}$ (100 mg) catalyst were added to PEG-400 (5.0 mL) with magnetic stirring. The reaction mixture was heated to 60 °C under 1 atm dioxygen pressure in a sealed tube. The progress of the reaction was monitored by TLC. After the disappearance of the starting material, the product was extracted in diethyl ether (10 mL × 3), concentrated under vacuum and purified by silica gel column chromatography, and eluted with 20% ethyl acetate in cyclohexane to yield the product as a colourless liquid (92 mg, 94%). ¹H NMR (300 MHz, CDCl₃): δ 7.48–7.53 (m, 2H), 7.58–7.64 (m, 1H), 7.85–7.88 (m, 2H) 10.00 (s, 1H). ¹³C NMR (75 MHz, CDCl₃): δ 128.39, 128.99, 129.70, 130.03, 134.45, 136.38, 192.38.

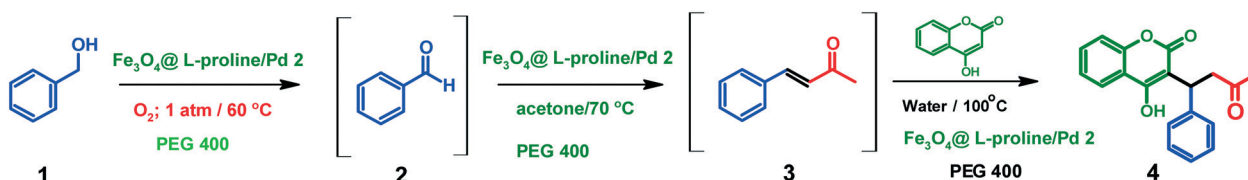
4-Chlorobenzaldehyde. Prepared as described for 2. Starting from 4-chlorobenzylalcohol (100 mg, 0.70 mmol), after purification with silica gel column chromatography eluted with 20% ethyl acetate in cyclohexane, a white solid was produced (79 mg, 80%), mp 46–47 °C. ¹H NMR (300 MHz, CDCl₃): δ 7.50–7.53 (m, 2H), 7.80–7.85 (m, 2H), 9.8 (s, 1H). ¹³C NMR (75 MHz, CDCl₃) δ 129.45 (2C), 130.90 (2C), 134.72, 140.92, 190.84.

p-Hydroxybenzaldehyde. Prepared as described for 2. Starting from 4-hydroxybenzylalcohol (100 mg, 0.80 mmol),

Table 7 One-pot conversion of benzyl alcohol and its derivatives to benzylideneacetone in the presence of $\text{Fe}_3\text{O}_4@L\text{-proline}/\text{Pd}2$ NCs under optimized reaction parameters^a


Sr. no.	-R	Time (h)	Expected product	Yield (%)
1	-NO ₂	60 + 24		No product
2	-H	60 + 24		47
3	-OH	60 + 24		No product
4	-CH ₃	60 + 24		52
5	-Cl	60 + 24		52
6	-OCH ₃	60 + 24		58

^a The detailed protocol is discussed in the Experimental section.

**Scheme 2** Synthesis of (±)-warfarin through 3-way catalysis in the presence of $\text{Fe}_3\text{O}_4@L\text{-proline}/\text{Pd}2$.

after purification with silica gel column chromatography eluted with 20% ethyl acetate in cyclohexane a light brown solid was obtained (88.5 mg, 90%), mp 110–113 °C. ¹H NMR (300 MHz, CDCl₃): δ 6.98–7.01 (m, 2H), 7.79–7.82 (m, 2H), 9.83 (s, 1H), 10.67 (brs, 1H). ¹³C NMR (75 MHz, CDCl₃) δ 116.66, 128.89, 132.54, 164.20, 191.31.

***p*-Methylbenzaldehyde.** Prepared as described for 2. Starting from 4-methylbenzylalcohol (100 mg, 0.82 mmol) after purification with silica gel column chromatography eluted with 20% ethyl acetate in cyclohexane, a colourless liquid was obtained (90 mg, 92%). ¹H NMR (300 MHz, CDCl₃) δ 2.41 (s, 3H), 7.30 (d, 2H), 7.75 (d, 2H), 9.94 (s, 1H). ¹³C NMR (75 MHz, CDCl₃) δ 21.81, 129.08, 134.20, 145.51, 191.93.

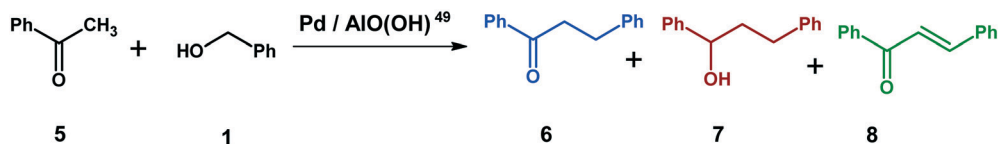
***p*-Methoxybenzaldehyde.** Prepared as described for 2. Starting from 4-methoxybenzyl alcohol (100 mg, 0.72 mmol), after purification with silica gel column chromatography eluted with 20% ethyl acetate in cyclohexane, a colourless liquid was obtained (76 mg, 78%). ¹H NMR (300 MHz, CDCl₃)

δ 3.82 (s, 3H), 6.94 (d, 2H), 7.76 (d, 2H), 9.82 (s, 1H). ¹³C NMR (75 MHz, CDCl₃) δ 55.58, 114.32, 129.94, 131.98, 164.62, 190.84.

***p*-Nitrobenzaldehyde.** Prepared as described for 2. Starting from 4-nitrobenzyl alcohol (100 mg, 65 mmol), after purification with silica gel column chromatography eluted with 20% ethyl acetate in cyclohexane, a yellow solid was obtained (15 mg, 15%), mp 102–104 °C. ¹H NMR (300 MHz, CDCl₃) δ 8.10 (d, 2H), 8.41 (d, 2H), 10.18 (s, 1H). ¹³C NMR (75 MHz, CDCl₃) δ 124.32, 130.51, 140.06, 151.12, 190.37.

4.4 One-pot synthesis of benzylideneacetone (3) from benzyl alcohol (1)

Benzyl alcohol (100 mg, 0.92 mmol) was added to PEG-400 (5 mL) and stirred for 10 min. Then, the catalyst $\text{Fe}_3\text{O}_4@L\text{-proline}/\text{Pd}2$ (100 mg) was added and stirred for 10 min. The reaction temperature was raised to 60 °C and the reaction



Scheme 3 Palladium-catalyzed coupling of acetophenone and benzyl alcohol in the presence of Park's catalyst.⁴⁹

was stirred for about 60 h under 1 atmosphere pressure of dioxygen. After the disappearance of the starting material (confirmed from the TLC plate), the dioxygen flow was stopped and the reaction was flushed with N₂ gas. At this time, acetone (5 mL) was introduced and the reaction mixture was stirred for 5 min under an inert atmosphere. The reaction vessel was sealed with a rubber septum and the mixture was stirred at 70 °C for about 24 h. The product was extracted in diethyl ether (10 mL × 3), concentrated and purified by column chromatography eluted with 25% ethyl acetate in cyclohexane to give 3 as a light-yellow low melting solid (64 mg, 47%). Rf 0.68 (1:4 ethyl acetate/cyclohexane). ¹H-NMR (300 MHz, CDCl₃) δ 2.36 (s, 3H), 6.70 (d, 1H), 7.38 (q, 3H), 7.49 (s, 1H), 7.52 (q, 2H). ¹³C NMR (75 MHz, CDCl₃) δ 27.49, 127.11, 128.28, 128.98, 130.55, 134.39, 143.51, 198.50.

4-Methoxybenzylideneacetone. Prepared as described for 3. Starting from 4-methoxybenzyl alcohol (100 mg, 0.72 mmol), after purification with silica gel column chromatography eluted with 25% ethyl acetate in cyclohexane a white low melting solid was obtained (84 mg, 58%). Rf 0.65 (1:4 ethyl acetate/cyclohexane). ¹H NMR (300 MHz, CDCl₃) δ 2.22 (s, 3H), 3.70 (s, 3H), 6.47 (d, 1H), 6.78 (d, 2H), 7.34 (d, 1H), 7.36 (d, 2H). ¹³C NMR (75 MHz, CDCl₃) δ 27.33, 55.32, 114.41, 124.93, 129.95, 143.22, 161.58, 198.29.

4-Chlorobenzylideneacetone. Prepared as described for 3. Starting from 4-chlorobenzyl alcohol (100 mg, 0.70 mmol), after purification with silica gel column chromatography eluted with 25% ethyl acetate in cyclohexane a tan low melting solid was obtained (66 mg, 52%). Rf 0.55 (1:4 ethyl acetate/cyclohexane). ¹H NMR (300 MHz, CDCl₃) δ 2.28 (s, 3H), 6.57 (d, 1H), 7.25 (d, 2H), 7.35 (d, 1H), 7.36 (d, 2H). ¹³C NMR (75 MHz, CDCl₃) δ 27.56, 127.42, 129.14, 129.38, 132.91, 136.21, 141.70, 197.88.

4-Methylbenzylideneacetone. Prepared as described for 3. Starting from 4-methylbenzyl alcohol (100 mg, 0.82 mmol), after purification with silica gel column chromatography eluted with 25% ethyl acetate in cyclohexane a yellow low

melting solid was obtained (68 mg, 52%). Rf 0.65 (1:4 ethyl acetate/cyclohexane). ¹H NMR (300 MHz, CDCl₃) δ 2.33 (d, 6H), 6.65 (d, 1H), 7.16 (d, 2H), 7.42 (d, 2H), 7.43 (d, 1H). ¹³C NMR (75 MHz, CDCl₃) δ 21.46, 27.37, 126.19, 128.28, 129.71, 131.64, 140.99, 143.53, 198.44.

4.5 One-pot synthesis of (±)-warfarin (4)

Benzyl alcohol (100 mg, 0.92 mmol) was added to PEG-400 (5 mL) and stirred for 10 min. Then the catalyst Fe₃O₄@L-proline/Pd 2 (100 mg) was added and stirred for 10 min. The reaction temperature was raised to 60 °C and the reaction was stirred for about 60 h under 1 atmosphere pressure of dioxygen. After the disappearance of the starting material on TLC, the flow of dioxygen was stopped and the reaction was flushed with N₂ gas. To this reaction mass, acetone (5 mL) was introduced and stirred for 5 min under an inert atmosphere. The reaction vessel was sealed with a rubber septum and stirred at 70 °C for about 24 h. Acetone was removed from the reaction mass under vacuum at 50 °C. At this time, 4-hydroxycoumarin (75 mg, 0.46 mmol) and water (5 mL) were added to the reaction mixture and stirred at 100 °C. After stirring for 12 h the reaction mass was cooled to room temperature and the catalyst was removed magnetically. The clear solution was dumped in 5 g ice. The product was filtered and recrystallized from acetone/water to give (±)-warfarin, (99 mg) as a white solid having 35% overall yield from benzyl alcohol. Melting point: 159–161 °C. ¹H NMR (300 MHz, CDCl₃) δ 2.04 (s, 3H), 3.29 (m, 2H), 4.89 (m, 1H), 6.99–7.40 (m, 8H), 7.82 (d, 1H). ¹³C NMR (75 MHz, CDCl₃) δ 30.19, 36.15, 46.85, 99.45, 115.62, 121.77, 124.04, 125.07, 125.22, 127.70, 128.12, 129.66, 147.40, 154.14, 164.25, 172.46, 209.50.

4.6 Production of (±)-warfarin at pilot plant

To a jacketed glass reactor of 1 L capacity, benzyl alcohol (10 g) and PEG-400 (500 mL) were added at ambient temperature and the mass was stirred for 10 min. To this was added the catalyst Fe₃O₄@L-proline/Pd2 (10 g) and the mixture was stirred for 10 min. The reaction mass was heated to 60 °C by applying hot water in the reactor jacket. This suspension was stirred for about 60 h at 60 °C under 1 atm pressure of dioxygen. After the disappearance of the starting material, the reaction was cooled to ambient temperature by applying chilled water in the jacket. Dioxygen was removed and the reaction was flushed with nitrogen. To this reaction mass, acetone (500 mL) was added and was stirred for 5 min under a nitrogen atmosphere. The reactor was closed and

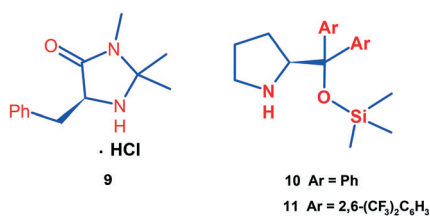


Fig. 4 MacMillan type imidazolidinone (9) and Jørgensen/Hayashi diarylprolinols (10, 11) as organocatalysts.

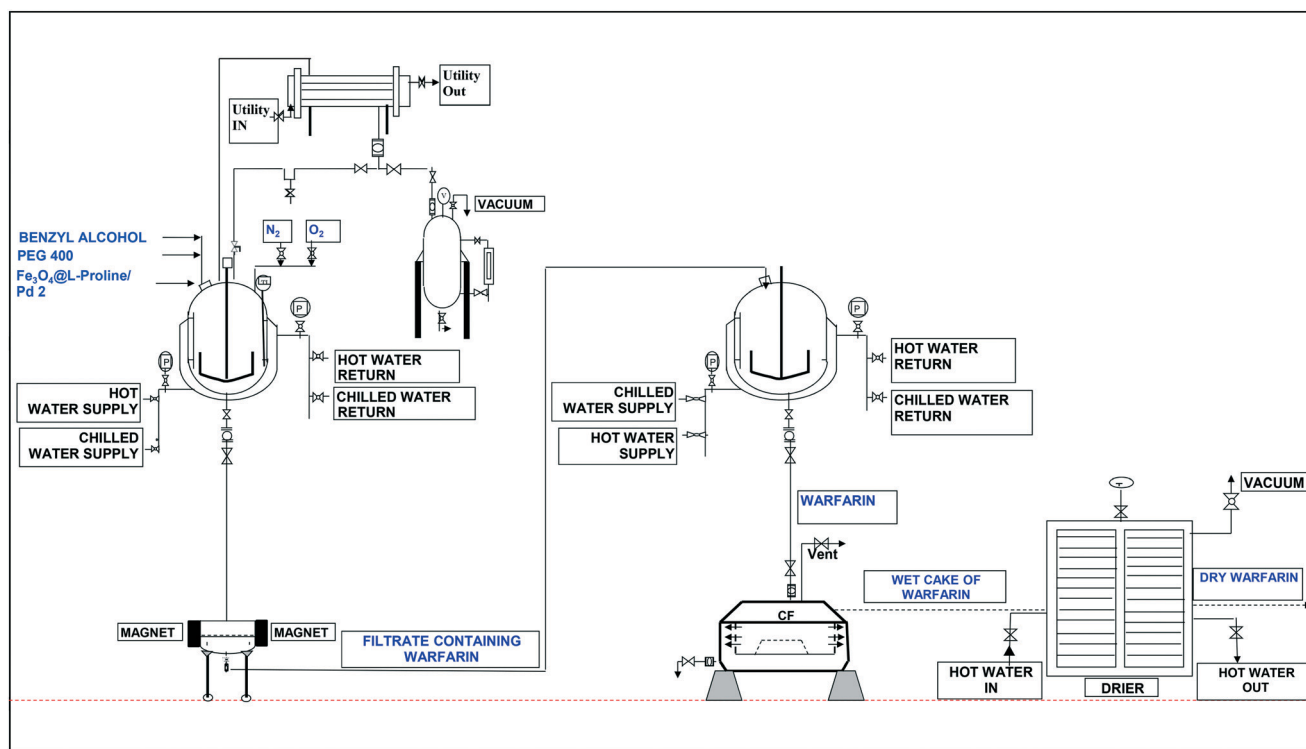


Fig. 5 Flow diagram for the pilot-scale production of (±)-warfarin from benzyl alcohol by the developed tandem process in the presence of $\text{Fe}_3\text{O}_4@L\text{-proline}/\text{Pd}$ NCs.

stirred at 70 °C for about 24 h. Acetone was removed from the reaction mass by applying a vacuum of about 100 millibar at 50 °C. The distilled acetone was collected in a receiver for further use. 4-Hydroxycoumarin (7.5 g), and water (500 mL) were added to the reaction mass and stirred at 100 °C. After stirring for 12 h the reaction mass was cooled to room temperature by applying chilled water circulation in the reactor jacket, and the catalyst was removed by a specially designed Neuch filter having magnetic bars. The clear solution was dumped in 500 g ice. The product was filtered and recrystallized from acetone/water to give (±)-warfarin (12.3 g) as a white solid with 43% overall yield from benzyl alcohol.

4.7 Characterization

An X-ray powder diffraction (XRD) pattern was obtained using an X-ray powder diffractometer (Philips X'pert MPD system) with $\text{Cu K}\alpha$ radiation, $\lambda = 0.15418$ nm. The morphology with elemental analysis of the samples was examined by FESEM (JEOL-JSM-7100F). The particle size determination with elemental mapping was carried out by TEM (JEOL-JEM-2100) at 200 kV. The samples were degassed at 80 °C prior to Brunauer–Emmett–Teller (BET) measurements. The BET specific surface area (S_{BET}) was determined by nitrogen adsorption (Micrometrics ASAP 2020, USA) via a multipoint BET method using the adsorption data

in the relative pressure (P/P^0) range of 0.0–1.0. The desorption isotherm was used to determine the pore-size distribution using the Barret–Joyner–Halenda (BJH) method, assuming a cylindrical pore model. The nitrogen adsorption volume at the relative pressure (P/P^0) range of 0.997 was used to determine the pore volume and average pore size. The FTIR (PerkinElmer, Spectrum Two) spectra of the synthesized products were obtained in the range of 400 to 4000 cm^{-1} . ^1H NMR and ^{13}C NMR spectra of the products were recorded on a Bruker Avance 300 MHz spectrometer using TMS as an internal standard in CDCl_3 . All the spectra are reported in the ESI.†

Abbreviations

$\text{Fe}_3\text{O}_4@L\text{-Proline}$ NPs L-Proline capped Fe_3O_4 nanoparticles
 $\text{Fe}_3\text{O}_4@L\text{-Proline}/\text{Pd}$ NCs L-Proline capped and Pd loaded Fe_3O_4 nanocomposites
 Reaction I Oxidation of benzyl alcohol to benzaldehyde
 Reaction II Aldol condensation of benzaldehyde with acetone

Conflicts of interest

There are no conflicts to declare.

Acknowledgements

HPS thanks the Science & Engineering Research Board (SERB), New Delhi, India for financial support under a sponsored scheme (No. EMR/2016/007638). The authors thank DST-FIST for providing the BET surface area measurement facility in the Department of Chemistry, Faculty of Science, The M. S. University of Baroda. We also thank Prof. A. V. Ramachandran for necessary suggestions and corrections in the manuscript.

References

- N. Halland, T. Hansen and K. A. Jørgensen, *Angew. Chem., Int. Ed.*, 2003, **42**, 4955–4957.
- J.-W. Xie, L. Yue, W. Chen, W. Du, J. Zhu, J.-G. Deng and Y.-C. Chen, *Org. Lett.*, 2007, **9**, 413–415.
- H. Kim, C. Yen, P. Preston and J. Chin, *Org. Lett.*, 2006, **8**, 5239–5242.
- R. M. de Figueiredo and M. Christmann, *Eur. J. Org. Chem.*, 2007, 2575–2600.
- T. Meinertz, W. Kasper, C. Kahl and E. Jahnchen, *Br. J. Clin. Pharmacol.*, 1978, **5**, 187–188.
- R. A. O'Reilly, *N. Engl. J. Med.*, 1976, **295**, 354–357.
- L. B. Wingard, R. A. O'Reilly and G. Levy, *Clin. Pharmacol. Ther.*, 1978, **23**, 212–217.
- T. A. Saleh, S. A. AL-Hammadi, I. M. Abdullahi and M. Mustaqeem, *J. Mol. Liq.*, 2018, **272**, 715–721.
- H. Chen, W. Liu and Z. Qin, *Catal. Sci. Technol.*, 2017, **7**, 2236–2244.
- Y. Li, X. Feng and Z. Li, *Catal. Sci. Technol.*, 2019, **9**, 377–383.
- G. Gedda, Y.-Y. Yao, S.-H. Chen, A. V. Ghule, Y.-C. Ling and J.-Y. Chang, *J. Mater. Chem. B*, 2017, **5**, 6282–6291.
- T. A. Saleh, *Desalin. Water Treat.*, 2016, **57**, 10730–10744.
- For a review of alcohol oxidation, see: A. M. F. Phillips, A. J. L. Pombeiro and M. N. Kopylovich, *ChemCatChem*, 2017, **9**, 217–246.
- J. Muzart, *Tetrahedron*, 2003, **59**, 5789–5816.
- G. Tojo and M. Fernández, in *Oxidation of alcohol to aldehyde and ketones: A guide to current common practice*, Springer, USA, 2006.
- K. Sato, M. Aoki and R. Noyori, *Science*, 1998, **281**, 1646–1647.
- B. M. Trost, *Science*, 1991, **254**, 1471–1477 (*Angew. Chem., Int. Ed. Engl.*, 1995, **34**, 259–281).
- J.-E. Backvall, R. L. Chowdhury and U. Karlsson, *J. Chem. Soc., Chem. Commun.*, 1991, 473.
- K. P. Peterson and R. C. Larock, *J. Org. Chem.*, 1998, **63**, 3185–3189.
- G.-J. ten Brink, I. W. Arends and R. A. Sheldon, *Science*, 2000, **287**, 1636–1639.
- J. A. Cella, J. A. Kelley and E. F. Kenehan, *J. Chem. Soc., Chem. Commun.*, 1974, 943.
- J. Muzart, *Tetrahedron*, 2003, **59**, 5789–5816.
- Z. Zhang, Y. Wang, M. Wang, J. Lu, C. Zhang, L. Li, J. Jiang and F. Wang, *Catal. Sci. Technol.*, 2016, **6**, 1693–1700.
- Y. Su, L. C. Wang, Y. M. Liu, Y. Cao, H. Y. He and K. N. Fan, *Catal. Commun.*, 2007, **8**, 2181–2185.
- M. Sono, M. P. Roach, E. D. Coulter and J. H. Dawson, *Chem. Rev.*, 1996, **96**, 2841–2887.
- S. Tareq, Y. H. T. Yap, T. A. Saleh, A. H. Abdullah, U. Rashid and S. M. Izham, *J. Mol. Liq.*, 2018, **271**, 885–891.
- D. I. Enache, J. K. Edwards, P. Landon, B. Solsona-Espriu, A. F. Carley, A. A. Herzing, M. Watanabe, C. J. Kiely, D. W. Knight and G. J. Hutchings, *Science*, 2006, **311**, 362–365.
- F. Zamani and S. M. Hosseini, *Catal. Commun.*, 2014, **43**, 164–168.
- X. Wang, G. Wu, N. Guan and L. Li, *Appl. Catal., B*, 2012, **115–116**, 7–15.
- T. K. Hollis and B. Bosnich, *J. Am. Chem. Soc.*, 1995, **117**, 4570–4581.
- T. Bach, *Angew. Chem., Int. Ed. Engl.*, 1994, **33**, 417–419.
- A. Erkkilä, I. Majander and P. M. Pihko, *Chem. Rev.*, 2007, **107**, 5416–5470.
- P. Clapés and J. Joglar, in *Modern Methods in Stereoselective Aldol Reactions*, ed. R. Mahrwald, Enzyme-Catalyzed Aldol Additions, Wiley-VCH Verlag GmbH & Co. KGaA, 2013, ch. 8., pp. 475–527.
- J. Wagner, R. A. Lerner and C. F. Barbas III, *Science*, 1995, **270**, 1797–1800.
- B. List, R. A. Lerner and C. F. Barbas III, *J. Am. Chem. Soc.*, 2000, **122**, 2395–2396.
- R. Jenkins and R. L. Snyder, *Introduction to X-ray Powder Diffractometry*, John Wiley & Sons, NY, 1996.
- K. S. W. Sing, D. H. Everett, R. A. W. Haul, L. Moscou, R. A. Pierotti, J. Rouquerol and T. Siemieniowska, *Pure Appl. Chem.*, 1985, **57**, 603–619.
- J. Yu, L. Zhang, B. Cheng and Y. Su, *J. Phys. Chem. C*, 2007, **111**, 10582–10589.
- E. Shah and H. P. Soni, *RSC Adv.*, 2013, **3**, 17453–17461.
- E. Shah, P. Upadhyay, M. Singh, M. S. Mansuri, R. Begum, N. Sheth and H. P. Soni, *New J. Chem.*, 2016, **40**, 9507–9519.
- M. Kakihana, T. Nagumo, O. Makoto and H. Kakihana, *J. Phys. Chem.*, 1987, **91**, 6128–6136.
- J. Chen, S. K. Spear, J. G. Huddleston and R. D. Rogers, *Green Chem.*, 2005, **7**, 64–82.
- E. Santaniello, A. Manzcocchi and P. Sozzani, *Tetrahedron Lett.*, 1979, **20**, 4581–4582.
- S. Chandrasekhar, C. Narsihmulu, B. Saritha and S. S. Sultana, *Tetrahedron Lett.*, 2004, **45**, 5865–5867.
- S. Chandrasekhar, C. Narsihmulu, S. S. Sultana and N. R. Reddy, *Org. Lett.*, 2002, **4**, 4399–4401.
- S. Chandrasekhar, C. Narsihmulu, S. S. Sultana and N. R. Reddy, *Chem. Commun.*, 2003, 1716–1717.
- Y.-Q. Cao, Z. Dai, R. Zhang and B.-H. Chen, *Synth. Commun.*, 2005, **35**, 1045–1049.
- S. Chandrasekhar, N. R. Reddy, S. S. Sultana, C. Narsihmulu and K. V. Reddy, *Tetrahedron*, 2006, **62**, 338–345.

- 49 M. S. Kwon, N. Kim, S. H. Seo, I. S. Park, R. K. Cheedra and J. Park, *Angew. Chem., Int. Ed.*, 2005, **44**, 6913–6915.
- 50 K. Motokura, D. Nishimura, K. Mori, T. Mizugaki, K. Ebitani and K. Kaneda, *J. Am. Chem. Soc.*, 2004, **126**, 5662–5663.
- 51 L. Yanan and C. Daoyong, *Chin. J. Chem.*, 2011, **29**, 2086–2090.
- 52 T. E. Kristensen, K. Vestli, F. K. Hansen and T. Hansen, *Eur. J. Org. Chem.*, 2009, 5185–5191.